J Mater Sci: Mater Med (2008) 19:239–247
DOI 10.1007/s10856-006-0032-y

Biomimetic Mg-substituted hydroxyapatite: from synthesis to in vivo behaviour

Elena Landi · Giandomenico Logroscino · Luca Proietti · Anna Tampieri · Monica Sandri · Simone Sprio

Received: 24 April 2006 / Accepted: 23 October 2006 / Published online: 28 June 2007

Abstract The incorporation of magnesium ions (in the range 5–10 mol% in respect to Ca) into the hydroxyapatite structure, which is of great interest for the developing of artificial bone, was performed using magnesium chloride, calcium hydroxide and phosphoric acid, as reactants. Among the synthesized powders, the synthetic HA powder containing 5.7% Mg substituting for calcium was selected, due to its better chemico-physical features, and transformed into granules of 400–600 μm, for biocompatibility tests (genotoxicity, carcinogenicity, toxicity, in vitro cytotoxicity and in vivo skin irritation-sensitization tests). In vivo tests were carried out on New Zealand White rabbits using the granulate as filling for a femoral bone defect: osteoconductivity and resorption were found to be enhanced compared to commercial stoichiometric HA granulate, taken as control.

Introduction

The processes of bone resorption and formation are tightly governed by a variety of systemic and local regulatory agents. In particular, the presence of trace elements affects bone formation and resorption through direct or indirect effects on bone cells or bone mineral.

The inorganic component of the bone tissue is non-stoichiometric apatite. This evidence stimulated the design and development of a new generation of synthetic resorbable apatite substitutes, which, simulating some properties of the biological phase, after implantation can actively participate to the bone regeneration, solving the problems caused by stoichiometric HA implants.

Biological apatites are poorly crystalline and contain cationic and anionic substitutions in the sites of the hydroxyapatite crystal structure; for this reason their composition are far from the typical HA stoichiometry $Ca_{10}(PO_4)_6(OH)_2$. Considering cationic substitutes, Mg ion is the most abundant, amounting typically around 6 mol%, in cartilage and bone tissue during the initial phases of osteogenesis, while it tends to disappear when the bone is mature [1]. Magnesium deficiency adversely affects all stages of skeletal metabolism, causing cessation of bone growth, decrease of osteoblastic and osteoclastic activities, osteopenia and bone fragility [2]. In addition to Mg, the natural inorganic component of bone is carbonate-substituted apatite; in particular, it contains higher amount of B-type carbonate (substituting for phosphate) compared to the A-type (substituting for hydroxyl): the A/B ratio is in the range 0.7–0.9, and this unbalance is bigger in the young bone [3]. The lower crystallinity-higher reactivity associated to the B-carbonate substitution compared to A-type [4] concurs to the higher reactivity of the young bone compared to the old one.

The preparation of synthetic Mg-doped hydroxyapatite is of great interest for the developing of artificial bone substitutes, which are characterised by high reabsorbability and can positively act at the same time as a source of Mg. The possibility to simply perform the B-carbonation in amount around the lower value of the carbonate biological

E. Landi (✉) · A. Tampieri · M. Sandri · S. Sprio
Institute of Science and Technology for Ceramics, National Research Council, Via Granarolo, 64, Faenza, RA 48018, Italy
e-mail: elena@istec.cnr.it

G. Logroscino · L. Proietti
Orthopaedic Department, Catholic University of Rome, largo F.Vito, 1, Rome 00168, Italy

range (3–8 wt% [5]) is also interesting, in particular if the synthetic apatite is implanted 'as synthesized', thus without undergoing any heat treatment or other processes that could modify its composition.

Synthetic apatite powders having low crystallinity-high reactivity can be prepared by wet chemical routes through control of the chemical precursors and process parameters (temperature, aging time, etc.). Furthermore, Mg ion was found to stimulate the nucleation of a high number of apatite nuclei whose crystallization becomes inhibited [4–7]. Many works are reported in literature since the 60s and 70s on the synthesis of calcium phosphates containing Mg. The characters of the products are widely different depending on the parameters including type of process, chemico-physical properties of the reactants, concentrations, temperature, aging, etc. [8]. Concerning specifically Mg-substituted hydroxyapatite [6, 7, 9–16], the syntheses are sometimes simply based on the immersion of HA in Mg nitrate solution (thus Mg introduction is attempted through ion exchange) [6, 9–13] or on the mixing of MgO and HA/TCP powders (in this case the doping aim is to improve the sintering) [15]. The Mg doping of apatite often is performed using magnesium nitrate as doping source. $MgCl_2$ was used in the synthesis of Mg-doped calcium deficient apatite starting from a mixture of Ca hydrogen phosphate and tetra calcium phosphate powders [7].

The present work reports on the effectiveness of Mg chloride (which is otherwise a constituent of the synthetic body fluid) in synthesizing Mg-substituted hydroxyapatite starting via the classical neutralization route involving calcium hydroxide and ortophosphoric acid precursors. This wet synthesis method was selected on the basis of previous experience in the synthesis of undoped hydroxyapatite powders, because the process parameters can be optimised to limit HPO_4^{2-} formation to undetectable levels and thus reducing or avoiding the formation of tricalcium phosphate. Considering that Mg tends to form TCP rather than HA, it is very important to avoid the formation of hydrogen phosphate ions to obtain Mg-HA. The biomimetic co-substitution of Mg and B-CO_3 in the HA structure was obtained performing the synthesis in air instead of inert atmosphere, thus utilising the CO_2 present in the atmosphere. The introduction of carbonate ions in the reaction mixture by bubbling carbon dioxide gas was otherwise demonstrated to enhance the A-site (hydroxyl) carbonation of synthetic Mg substituted as well as stoichiometric hydroxyapatites [9, 17, 18].

Materials and methods

Synthesis of powders

Mg-doped hydroxyapatite (MgHA) powders were prepared at 40 °C in air atmosphere by dropping in 3 h 600 mL of an aqueous solution containing 88.8 g of H_3PO_4 (Aldrich, 85% pure) into basic suspensions consisting of 100 g $Ca(OH)_2$ (Aldrich, 95% pure) and different amounts of $MgCl_2 \cdot 6H_2O$ (Merck, A.C.S., ISO) in 1,000 mL of water. A series of powders having varying Mg/Ca ratios were synthesized from the starting basic suspension containing Mg molar fraction $X_{Mg} = Mg/(Mg + Ca) = 0.15$, 0.20, 0.25, 0.30. Each precipitation product was aged for 24 h at 25 °C then washed and filtered 3 times, freeze dried, and finally sieved at 150 μm.

The specific surface area of the powders was measured by the Brunauer–Emmett–Teller (B.E.T.) gas adsorption method (Sorpty 1750, Carlo Erba, Milano, Italy). The particle size distribution of the powders was analysed by sedimentography (Sedigraph 5100, Micromeritics, Norcross, GA) after ultrasonic dispersion for 10 min. The morphology of the powders and granulates was examined by scanning electron microscopy (SEM; Stereoscan 360, Leica, Cambridge, UK). Inductively coupled plasma-optical emission spectrometry (ICP-OES) analysis (Liberty 200, Varian, Clayton South, Australia) and Fourier transformed infrared (FTIR) spectroscopy (Thermo Nicolet-Avatar 320 FT-IR) were performed to determine HA stoichiometry deviations, in particular Mg/Ca molar ratio and carbonate substitutions. Carbon elemental analysis (LECO C/S, Leco Corporation, St. Joseph, Michigan, USA) and simultaneous thermal analysis (STA 409 Netzsch Geraetebau GmbH, Selb, Germany) were used to estimate the carbonate content of the powders. X-ray diffraction (Cu Kα radiation, Miniflex Rigaku, Tokyo, Japan) was performed to evaluate the crystallinity and phase composition of the samples.

Zeta-potential and conductivity were measured in function of pH by an electroacoustic technique, using an electrokinetic sonic amplitude (ESA) measurement apparatus (Acoustosizer, Colloidal Dynamics, Sydney, Australia). A suspension sample was prepared by ball milling the powder for 1 h in 10^{-2} M KCl solution to maintain a constant ionic strength. A fixed concentration of 1 vol% solid was used and the suspension, placed in the measurement cell, was kept under constant stirring at 25 °C. An automatic titration software was used to measure the Zeta potential and conductivity as a function of pH (1 M HNO_3 and 1 M KOH were used to adjust the pH). The isoelectric point (IEP) was identified as the pH axis crossing point. The conductivity curve versus pH allowed to compare the solubility behaviour of the MgHA powder with that of stoichiometric HA.

One of the synthetic MgHA powders ($X_{Mg} = 0.15$ in the starting suspension, producing 5.7 mol% Mg-substituted HA) was granulated (granule size 400–600 μm) by spraying distilled water and sieving. The solubility behaviour of 3 g of MgHA granules in Hank's balanced salt solution

(Sigma code: H9394) at $T = 37$ °C under dynamic conditions (the total SBF volume flowed through the material per day was 300 mL) was evaluated and compared with that of commercial stoichiometric HA granules (Fingranule, Fin-Ceramica Faenza Spa, Italy) of similar dimensional range.

Biocompatibility testing

The biocompatibility of the 5.7 mol% Mg-HA granules was evaluated in terms of genotoxicity, carcinogenicity and toxicity (UNI EN 30993-3 protocol), and cytotoxicity (UNI EN 30993-5 protocol). Subcutaneous irritation and sensitisation tests in vivo (UNI EN 30993-10 protocol) were also performed. All testings were performed in a certified laboratory (Biolab Spa, Vimodrone, Milan, Italy).

Twelve adult male NZ white rabbits, each weighing approximately 3 kg, were used for the in vivo evaluation. The animal experiments were approved by the Ethic Committee of the Catholic University of Rome and followed local and international guidelines for the care and use of laboratory animals. Each animal was anesthetized by intramuscular injection of ketamine hydrochloride (50 mg/kg) and Medetonidina (0.3 mg/kg). Anesthesia was maintained by additional boluses of ketamine, as needed. Following shaving and disinfecting the distal portion of each femur, the femoral condyles were exposed by incision and a 5 mm diameter hole drilled through the condylar surface to a depth of 10 mm. A manual drill was used for all drillings to minimize osteonecrosis at the bone-material interface. The hole was rinsed by irrigation with physiologic saline solution and then the ceramic granules were inserted into the hole by a press-fit technique. The periosteoum, subcutaneous tissue, and skin were closed in layers by suture. The animals were divided into 2 groups: 6 rabbits (12 limbs) were implanted with 5.7% Mg-substituted HA granules, and the other 6 rabbits were implanted with stoichiometric HA granules (Fingranule, Fin-Ceramica Faenza spa, Italy). Antibiotic prophylaxis with ceftazidime was started 30 min before surgery and continued with 10 mg/kg per day for 2 days. After sacrifice at 4, 8 and 12 weeks postoperatively, the specimens and surrounding tissue were harvested and embedded in poly methyl methacrylate embedded (Technovit 7200, Bioptica). Sections were cut longitudinal to the bone tunnel axis and stained with toluidine blue. Histology of the bone–ceramic interface was evaluated using a light microscope (Carl Zeiss Axioskop 40) coupled to a video camera. Histomorphometric analysis was done by image analysis software (Axiovision 3.1). The length (ML) and area (MA) of the total material implanted were measured. The length of the total bone-material direct contact (BML) was measured and the percentage of bone apposition at the implant surface (%BMC) was determined. This was defined as the percentage of the total material length at which there was direct bone-to-implant contact.

The extent of tissue penetration into the ceramic granules was measured as (i) the length of tissue penetration (PTP-L) expressed as a percentage of the diameter of the bone tunnel section; (ii) the total area of bone (PTP-A), expressed as a percentage of the total area of bone plus non-bone tissue, in radial bone tunnel in which the material is contained.

Radiographic examination was also performed at time equals 4, 8 and 12 weeks.

Results and discussion

Chemico-physical properties of the MgHA powders

The actual Mg/Ca molar ratio detected by ICP-OES analysis in the synthesized powders was approximately in the range 6–14 mol%, (Table 1), i.e. around and over the maximum amount present in the biological apatite.

The low temperature of the synthesis and the presence of magnesium ions acted with synergic effect to make the apatite nuclei smaller and to inhibit the crystallization process: XRD analysis pointed out that the Mg-doped powders were pure apatitic phases, which, compared to stoichiometric hydroxyapatite, showed lower crystallinity extent Xc, as much more as X_{Mg}, and consequently the actual Mg-doping, increased (Fig. 1a, c): the XRD profile of the Mg-HA powder was similar to that of natural apatite (Fig. 1d). The crystallinity grade Xc of the powders was evaluated on the basis of an experimental method elsewhere reported [19], which was developed and found to be applicable for apatites with nanosized crystallites; briefly, Xc, corresponding to the fraction of crystalline phase present in the examined volume, was evaluated by the relation:

$$Xc \approx 1 - (V_{112/300}/I_{300})$$

where I_{300} is the intensity of (300) reflection and $V_{112/300}$ is the intensity of the hollow between (112) and (300) reflections, which completely disappears in non-crystalline samples.

The specific surface area of the doped powder, increased progressively up to ~125 m^2/g with increasing the starting X_{Mg} from 0.15 to 0.25 (Table 1). The particle (agglomerate) size distribution (detected by sedimentography) together with SEM analysis pointed out that nanosized primary particles aggregated each other more and more as the Mg doping of the powder increased (mean particle size ≈1 μm and ≈2.5 μm respectively for 5.7%Mg- and 13.3% substituted HA). SEM analysis of the Mg-doped HA

Table 1 Chemico-physical characteristics of the Mg-doped apatite powders

X_{Mg} starting solution	0.15	0.20	0.25	0.30
$(Mg/Ca)_{mol}$%	5.7	7.5	13.3	13.7
Mg doping wt%	0.7	1.8	3.1	3.2
s.s.a (m^2/g)	88	105	125	64

showed primary particles of about 1/5 or less of the particle dimension of stoichiometric hydroxyapatite (which typically was about 160 nm), thus in the range of interest for human tissues [4]. The density of Mg-HA powders, evaluated by helium pycnometry, was in the range 2.7–2.9 g/cm^3, lower values compared to that (3.16 g/cm^3) of stoichiometric HA. This was expected as a consequence of the process of ionic substitutions in the apatite structure, which is accomplished by the increase of the number of structural defects. The specific surface area values were consistent with nanometric particle sizes, i.e. in accordance with SEM results but respectively about 2 order of magnitude lower than the mean (agglomerate) particle size values found by sedimentography.

The Rietveld refinement method of the XRD data pointed out that for $X_{Mg} = 0.20$ the limit value of Mg entering in the structure as Ca substitute (~10% [10, 20]) was almost reached: the Mg amount substituting for calcium was in fact evaluated as ~7–8%, which is moreover in very good agreement with the value (7.5) found by ICP spectroscopy (Table 1). In the powders prepared starting from $X_{Mg} = 0.25$ and 0.30, Mg was thus necessarily present also in the hydrated layer and/or amorphous phase, in amount at least ~3–4% (i.e. the difference between the Mg amounts determined by ICP and the maximum amount of Mg that can enter in the structure: about 10%). Such considerations were supported and confirmed by cathodoluminescence spectroscopy, which was able to assign to specific and separate peaks the different physico-chemical characteristics of the apatite powders (crystallinity, Mg substituted in the lattice, Mg segregated outside the lattice in the hydrated layer) making possible comparative considerations about the powders on the basis of the peak intensity differences [21].

From thermogravimetric analysis detection and in agreement with the Carbon elemental analyzer, the carbonate amount was quantified as about 2 wt% and 3 wt% respectively in the 5.7%- and 7.5%-MgHA powders, values which are around the lower limit of the content range of the biological apatite. This result is in agreement with previous findings [4] about the ability of Mg and CO_3 in stimulating each other to enter in the apatite structure when simultaneously present in the synthesis environment. The B-carbonate amounts (2 and 3 wt%) were also in agreement with the (Ca + Mg)/P molar ratio values ~1.72 and ~1.79 determined by ICP analysis respectively for the 5.7%Mg-HA and 7.5%Mg-HA, since it is well known that carbonate substitutions in the B-site cause specific positive deviations of the molar ratio from the stoichiometric HA value (1.67). Various findings suggested the highly (>13%) Mg-doped powders being probably affected with not neglectable amounts of HPO_4^{2-} ions substituting together with CO_3^{2-} for phosphate ions in the apatite structure, in particular: lower molar ratio value than expected; a small weight loss associated to an endothermic reaction at ~400 °C, that is assignable to the condensation reaction of hydrogen phosphate ions, and which was more evident for the highly Mg doped HA; the increase of destabilization of the apatite

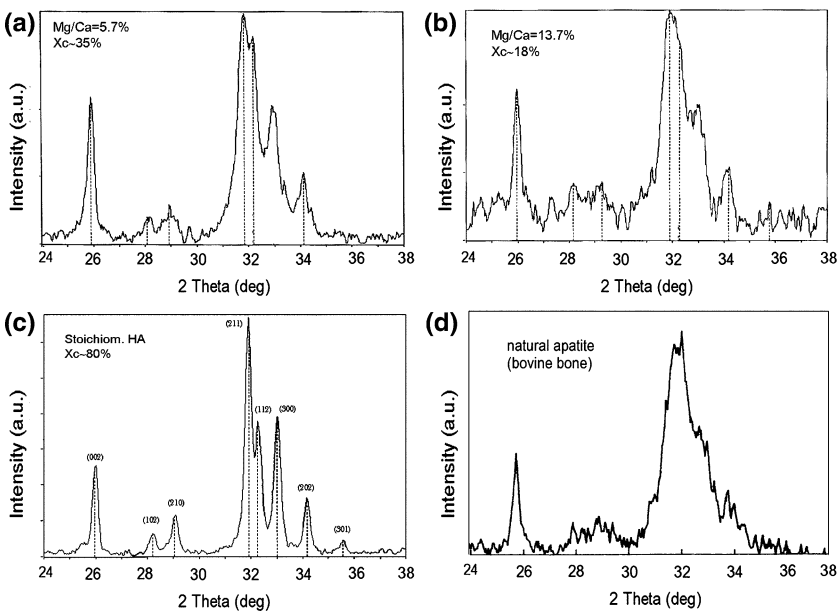

Fig. 1 XRD analysis of the HA powders substituted with 5.7 mol% Mg/Ca (**a**) and 13.7 mol% Mg/Ca (**b**) compared to highly crystalline stoichiometric HA (**c**) and biological apatite (**d**) powders

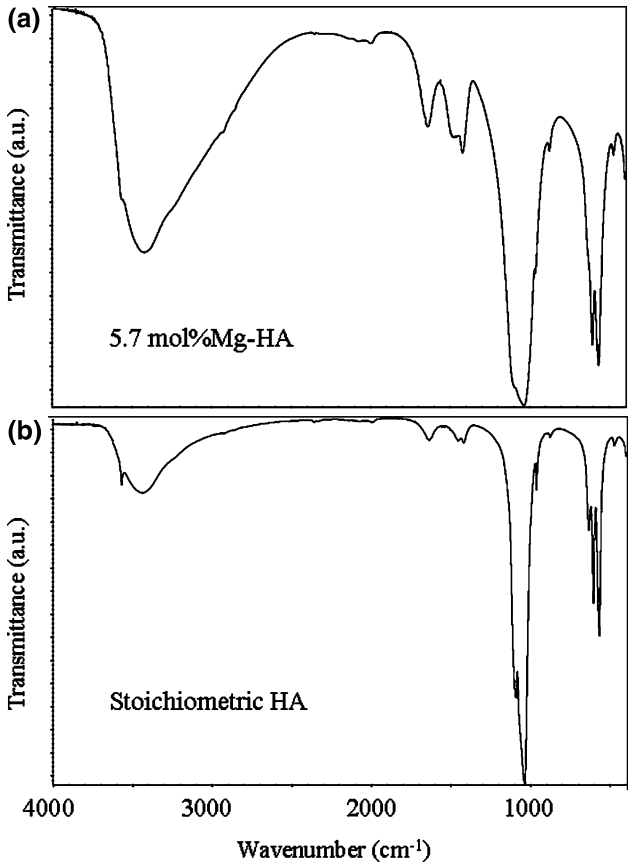

Fig. 2 FTIR analysis of the 5.7 mol% Mg substituted HA powder (**a**) showing broaden profile as well as evident carbonation signals compared to stoichiometric HA (**b**)

structure causing TCP formation after heating (at 1,250 °C the Mg-doped powders formed 20, 26, 56 and 61 vol% of β-TCP respectively with the increase of the Mg doping).

FTIR analysis of the MgHA powders gave broaden spectra, compared to stoichiometric HA. Together with the phosphate bands at 980–1,100 cm^{-1} and 560–600 cm^{-1}, the presence of both the absorbed and the occluded water was detected, being respectively referred to the broad band around 3,500 cm^{-1} and to the peak at 1,640 cm^{-1}. Moreover, the typical signals of B-carbonation (substitution in the phosphate site: CO_3^{2-} stretching signals at ~1,410 and ~1,450 cm^{-1} and bending peak at ~873 cm^{-1}) were detected, in agreement with the results obtained by the other analyses; in Fig. 2a, b the comparison between the 5.7 mol%Mg-HA and stoichiometric HA is shown.

It is well known that the surface features of the powder greatly influence the biomimetism of the apatites since they affect the protein adhesion process and in turn the cell adhesion and proliferation. An investigation performed using under vacuum/gas adsorbed (Carbon monoxide) FTIR spectroscopy, demonstrated that different kinds of water are present in apatites and they are differently bonded to the HA surface and bulk, depending also on the surface cations (Ca^{2+} and Mg^{2+}) [22]. On the other hand TEM observations of the powders pointed out that stoichiometric HA microcrystals were limited by defined planes, edges and corners. In the case of MgHA powder, ordered crystals were found in the bulk and an amorphous layer near the surface (Fig. 3a–d).

On the basis of the results of the chemico-physical analyses the 5.7% Mg-substituted HA powder was selected for further tests, i.e. solubility, in vitro and in vivo evaluations. The powder was transformed into granules of 400–600 μm, following the same granulation procedure used for Fingranule HA. The SEM analysis (Fig. 4a–c) pointed out that the granules of 5.7 mol%Mg-HA and Fingranule HA materials, which were morphologically similar at low magnification, were on the contrary formed by grains with dimensions ranging in the tens nm scale in the case of MgHA and one order of magnitude over in the case of stoichiometric HA (Fingranule). This finding was in agreement with the primary particle dimensions of the 5.7%Mg-substituted HA powder and it was expected, since the peculiar granulation process do not alter the intrinsic chemico-physical properties of the apatite material. The comparative solubility test of the Mg-HA and (Fingranule) HA granulates was performed in Hank's balanced salt solution in dynamic conditions at $T = 37$ °C. Strong ion release was detected in the case of the Mg-substituted HA (Table 2), while the dissolution of stoichiometric HA (Fingranule) was very limited with no change during the first week (as expected, considering the very low value of Kps = 2×10^{-58}, widely reported in literature). All the chemical-physical characteristics of the Mg-doped apatite, as Mg-doping, B-type CO_3-doping, low crystallinity and specific surface area, which influence each other, concurred to enhance the solubility of the material. The solubility difference among non-stoichiometric and stoichiometric HA, was otherwise highlighted in advance comparing the electroacoustic behaviour of the powders' suspensions, before performing the solubility test of the granules in Hank's solution. In the case of 5.7 mol%Mg-doped HA (Fig. 5) the conductivity curve goes up moving towards the acidic pH range (detecting acidic dissolution) starting from pH value close to the physiological one (7.4), i.e. at less acid pH value, compared to stoichiometric HA (pH~6.5). From Z potential measurements (Fig. 5) the shift of pH_{IEP} toward basic pH was detected in the case of 5.7 mol%Mg-HA compared to stoichiometric HA (pH_{IEP} ~ 7), and was determined by the establishment of a cationic specific adsorption and can be due either to higher content of cations leached from the surface complex and/or to the presence of carbonate group, i.e. anion which shows a stronger affinity for cations.

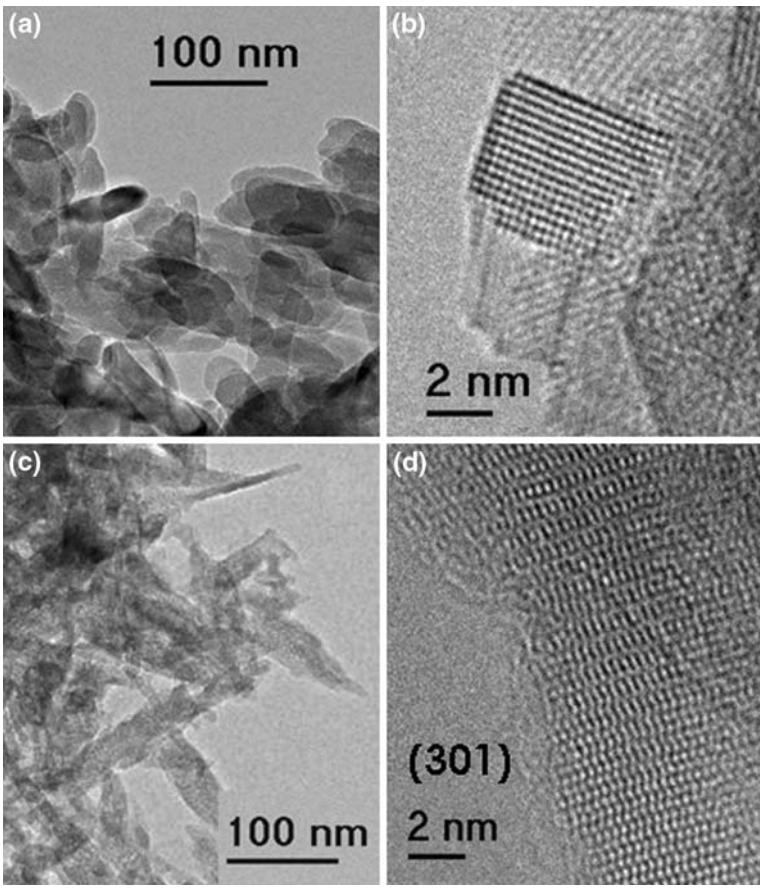

Fig. 3 TEM analysis of stoichiometric HA powder (**a**, **b**) and 5.7 mol% Mg-substituted HA powder (**c**, **d**) showing the different morphological and microstructural features

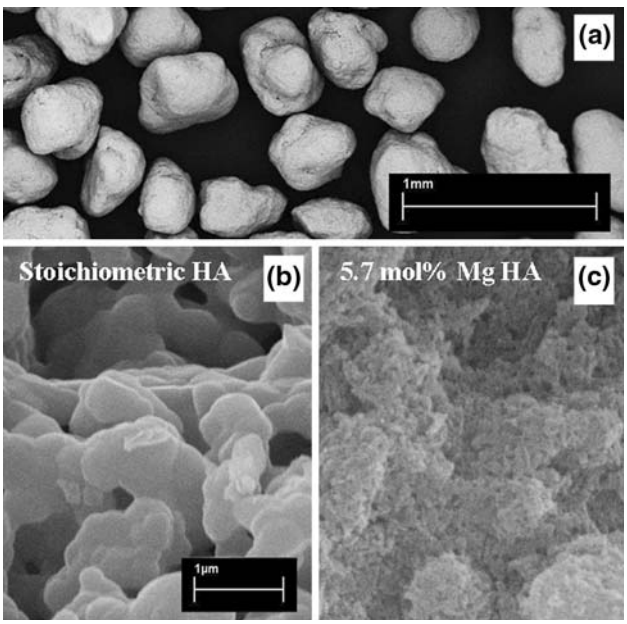

Fig. 4 SEM analysis of the granulate. At low magnification the granulates are morphologically indistinguishable and look as in (**a**) while at high magnification the differences are evident: stoichiometric HA (**b**) and 5.7 mol% Mg-doped (**c**) granulates

In vitro and in vivo tests

The 5.7 mol%Mg-doped HA granules showed no genotoxicity, carcinogenicity and cytotoxicity. Also the skin irritation-sensitisation tests were negative. The biocompatibility of the material was thus demonstrated.

Eighteen specimens of the femur implant were available for the study in vivo. Major complication like fracture, infection and intraoperatory death occurred in five cases. Intraoperatory death samples were used as T0 (0 days) samples. In one case a fracture occurred at the 15th day and the limbs were explanted and examined.

Light microscopy

Sections of the samples at T0 revealed the presence of a gap between both the materials and the original bone. The gap length was variable from 50 to 504 μ (Fig. 6). In both the materials the bone formation was intense at 15 days and fine bone trabeculae were observed at 4 weeks (Fig. 7a, b). A slight more evidence of bone invasion was observed in the stoichiometric HA samples in the first month. Bone formation with osteoid and woven bone in the

Table 2 Solubility test results: ICP-AOS analysis of cations released from 5.7 mol% Mg-HA granulate and Fingranule HA in Hank's balanced salt solution every 24 h during the first week and after 2, 3, and 4 weeks

Material	Time									
	Ion (ppm)	24 h	48 h	72 h	96 h	120 h	144 h	168 h	2 weeks	3 weeks	4 weeks
HA	Ca^{2+}	0.02	0.01	–	0.02	–	–	0.01	–	–	–
MgHA	Ca^{2+}	1.50	0.59	0.42	0.43	0.36	0.43	0.33	0.25	0.26	0.25
	Mg^{2+}	11.21	3.20	2.04	1.72	1.43	1.39	1.12	0.72	0.59	0.34

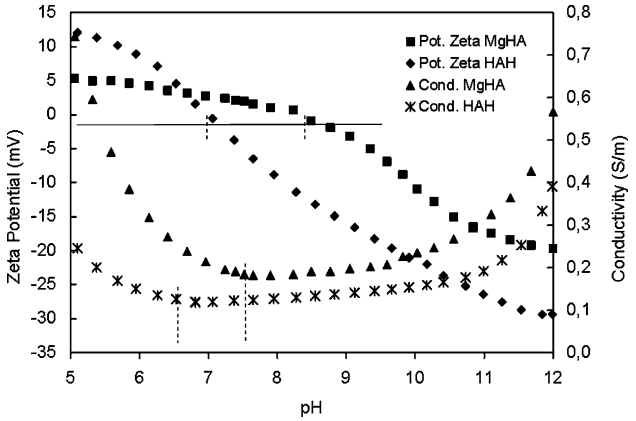

Fig. 5 Zeta potential and conductivity versus pH for 5.7 mol% Mg-doped and stoichiometric HA

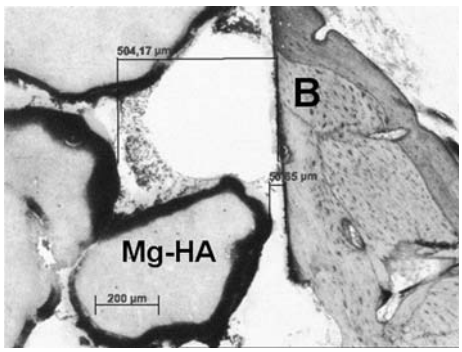

Fig. 6 Time 0 sample of Mg-HA granules. The press-fit implantation of the material into the bone hole achieved a 4.6% of %BMC. The gap between the host bone (B) and the implanted granules (Mg-HA) varied between 50 and 500 μ (Toluidine Blue-light microscopy 20 ×)

zone next to the material surface was present in all the granules. Osteoblasts depositing osteoid directly on the granules surfaces were observed. Delamination and fragmentation of the granules were mostly evident in the Mg-substituted HA group.

At 8 weeks, bone remodelling (osteoclastic resorption/osteoblastic osteogenesis) was observed around both the materials. Mature lamellar bone has begun to substitute the primitive woven bone as confirmed by polarized light

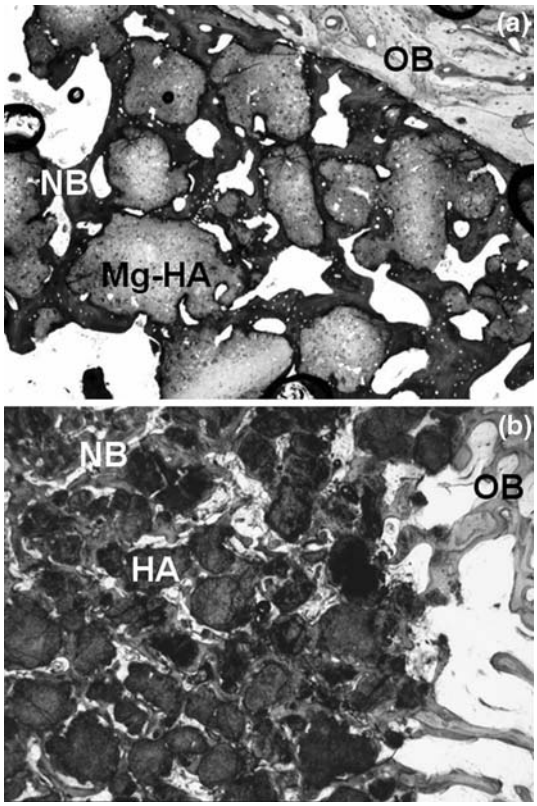

Fig. 7 (**a**) Mg-HA granules at 1 month: Bone invasion proceeded from the outer old bone (OB) to the inner part of the material (Mg-HA). At this stage the PTP was 100% completed by woven, immature newly formed bone (NB). (**b**) the same result was observed for the control samples (HA). (Toluidine Blue-light microscopy 4 ×)

microscopy. Vascular invasion of the macropores was present in the Mg-substituted HA group samples.

At 12 weeks most of both the materials granules were completely surrounded by lamellar bone tissue. At higher magnification the histological analysis revealed that the osteogenesis process is maintained by an endosteal apposition of osteoblastic cells on bone trabeculae next to the granules. Although at this follow-up the signs of granules degradation and delamination proceed, the process of resorption of both the materials was partial, but was mostly present in Mg-HA samples (Fig. 8a, b).

Histomorphometry

Bone invasion increased progressively over the time in both the materials. At 15 days the Mg-doped HA demonstrated a relatively high PTP-L (min: 42.1% max: 80.7%; mean 61.4%) and PTP-A (85.5%); these values were comparable to stoichiometric HA. Bone invasion of the granules was complete (100%) at 1 month of follow-up in all the samples of both the materials.

%BMC increased progressively over the time as showed in Fig. 9; a certain evidence of bone-material contact (%BMC) was found even at T0, resulting from the compression of the material into the drilled hole; at 1 month of follow-up %BMC was higher for stoichiometric HA samples. On the contrary at 2 and 3 months of follow-up a significant larger amount of %BMC was observed in the Mg-doped samples. The total area (MA) and the total length (ML) of the materials were decreased progressively over the time. The mean MA and ML per single granule were decreased respectively of 52.6% and 47.2% for Mg-doped HA and of 38.9 and 23.8 for stoichiometric HA from T0 to 3 months.

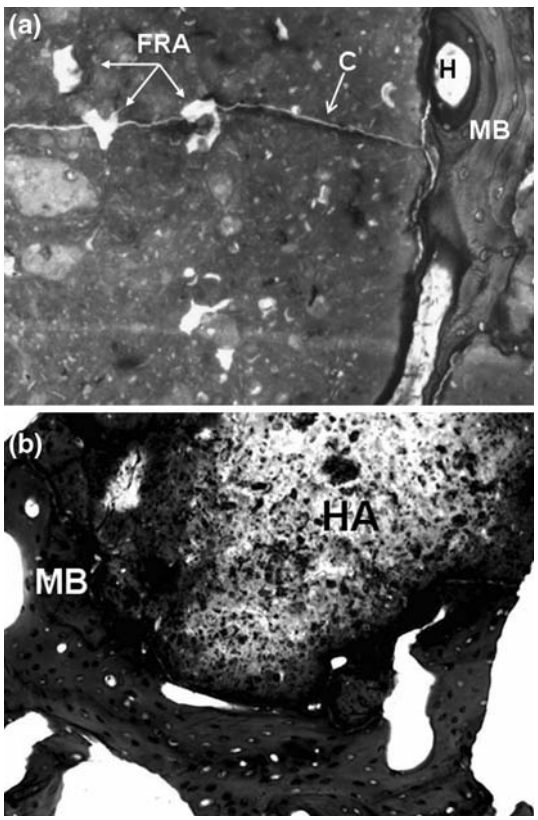

Fig. 8 (**a**) Mg-HA granules at 3 months of follow-up: while the bone remodelling progresses, mature bone (MB) with lamellar bone apposition and Havers canals formation (H) were observed around and in contact with the material. At the same time, focal resorptive areas (FRA) inside the Mg-HA appear. The granules fragility due to degradation was demonstrated by the frequent presence of cracks (C) inside the material in conjunction with the FRA. (**b**) the control samples (HA) showed mature bone (MB) around the granules without signs of observable degradation. (Toluidine Blue-light microscopy 40 ×)

Radiology

At 15 days the radiographic analysis of both the materials showed a thin line of radiolucency at the bone-material interface that disappeared completely between the 4th and the 8th week. At this follow-up the reorganization of the trabeculae was also observed. These findings correspond to the histological observation of incorporation of the granules and the trabecular bone formation from the outer to the inner part of the materials. At 3 months the Mg-HA and the stoichiometric HA were well integrated in the host bone without any sign of osteolysis or adverse reaction.

Both the materials revealed to be very osteoconductive and effective as bone substitutes. At 1 month both the HA have demonstrated a complete bone ingrowth, (PTP 100%) by woven bone. Between the 2nd to the 3rd month mature bone substituted the woven bone and the bone remodelling was completed at the 3rd month. Stoichiometric HA showed faster bone invasion at 1 month, while Mg-doped HA demonstrated a greater amount of bone in contact to the material (%BMC) at 2 and 3 months and an increased amount of resorption of the material. This degradation was not limited to the granule peripheries but it was also present in the centre of the granule, leading a decrease of both the dimension and total surface area of the material. These findings were confirmed by histomorphometry assessments and by the delamination, fragmentation and neo-vascular invasion observed at the light microscopy analysis.

The results of the in vivo tests are in agreement with the chemico-physical properties of the two materials. The higher solubility of the Mg substituted HA was well established through the electroacoustic technique and the solubility test in synthetic body fluid. The nanodimensions of the Mg-HA primary particles, provide a larger surface

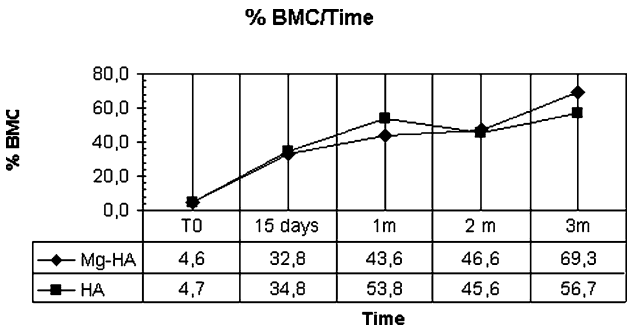

Fig. 9 %BMC (Percentage of Bone-Material Contact) for Mg-HA and stoichiometric HA granules at different periods of follow up

area for dissolution. The faster bone invasion found in stoichiometric HA granules after 1 month can be due to the surface morphology of the HA granules which, being formed by agglomerating bigger primary particles compared to Mg-HA, presents macropores more well defined on the granule surface; in fact the granulation process itself tends to compact each other the powder particles more and more the smaller they are. The surface features allow more easily osteoinvasion toward the centre of the stoichiometric HA granule. In the case of Mg-HA granule, the surface is more compacted due to the nanosize of the starting powder particles and the resorption initially prevails, but it is at the same time necessary to increase the channels that allow bone cell penetration. After that, the biomimetic features (composition, nanoparticles, surface characteristics) of the Mg-HA reflect in higher amount of bone in contact to the material, compared to stoichiometric HA.

Conclusions

Synthetic HA doped with different Mg amount (6–14% of Ca moles) were prepared via wet-chemical synthesis. The ion dopings and the synthesis conditions of the 5.7 mol% Mg-substituted HA made the apatite biologically like in term of composition, morphology, crystallinity and was selected for further tests after a granulation process.

The 5.7 mol%Mg doped HA granulate was biocompatible since it showed no genotoxicity, carcinogenicity and cytotoxicity.

Mg-HA granulate demonstrated to be comparable or better than traditional HA as a bone substitute when tested in vivo. In particular Mg-HA showed greater osteoconductivity over the time and higher material resorption, compared to stoichiometric HA. The results obtained are explained on the basis of the chemico-physical-morphological properties and solubility of the Mg-HA granules. MgHA initially gives slower bone ingrowth into granules but once bone gets in, finds more favourable conditions for its growth due to the composition, nanodimension and surface characteristics of the MgHA material.

Acknowledgements Authors want to thank Fin-Ceramica Faenza S.p.a.—Italy for supplying the Fingranule material.

References

1. A. BIGI, E. FORESTI, R. GREGORIANI, A. RIPAMONTI, N. ROVERI and J. S. SHAH, *Calcif. Tissue Int*. **50**, (1992) 439
2. M. PERCIVAL, *Appl. Nutr. Sci. Rep*. **5** (1999) 1
3. C. REY, V. RENUGOPALAKRISHNAN, B. COLLINS and M. GLIMCHER, *Calcif. Tissue Int*. **49** (1991) 251
4. R. Z. LE GEROS, Calcium phosphates in oral biology and medicine. In *Monographs in oral science* edited by H. Myers Karger, vol. 15 (Basel: AG Publishers, 1991), p. 82
5. F. C. M. DRIESSENS, *Bioceramics of Calcium Phosphates*. (Boca Raton, FL: CRC Press, 1983), p. 1
6. A. BIGI, G. FALINI, E. FORESTI, M. GAZZANO, A. RIPAMONTI and N. ROVERI, *J. Inorg. Biochem*. **49** (1993) 69
7. K. S. TENHUISEN and P. W. BROWN, *J. Biomed. Mater. Res*. **36** (1997) 306
8. P. T. CHENG, J. J. GRABBER and R. Z. Le GEROS, *Magnesium* **7**(3) (1988) 123
9. I. R. GIBSON and W. BONFIELD, *J. Mat. Sci. Mat. Med*. **13** (2002) 685
10. A. BIGI, G. FALINI, E. FORESTI, M. GAZZANO, A. RIPAMONTI and N. ROVERI, *Acta Cryst.* **B52** (1996) 87
11. R. N. CORREIA, M. C. F. MAGALHAES, P. A. A. P. MARQUES and A. M. R. SENOS, *J. Mat. Sci. Mat. Med*. **7** (1996) 501
12. M. A. FANOVICH, M. S. CASTRO and J. M. PORTO LOPEZ, *Ceram. Int*. **25** (1999) 517
13. A. BIGI, F. MARCHETTI, A. RIPAMONTI and N. ROVERI, *J. Inorg. Biochem*. **15** (1981) 317
14. S. BARAVELLI, A. BIGI, A. RIPAMONTI and N. ROVERI, *J. Inorg. Biochem*. **20** (1984) 1
15. H. S. RYU, K. S. HONG, J. K. LEE, D. J. KIM, J. H. LEE, B. S. CHANG, Dh. LEE, Ck. LEE and S. S. CHUNG, *Biomaterials* **25** (2004) 393
16. S. R. KIM, J. H. LEE, Y. T. KIM, D. H. RIU, S. J. JUNG, Y. J. LEE, S. C. CHUNG and Y. H. KIM, *Biomaterials* **24** (2003) 1389
17. E. LANDI, A. TAMPIERI, G. CELOTTI, L. VICHI and M. SANDRI, *Biomaterials* **25** (2004) 1763
18. I. R. GIBSON and W. BONFIELD, *J. Biomed. Mater. Res*. **59** (2002) 697
19. E. LANDI, A. TAMPIERI, G. CELOTTI and S. SPRIO, *J. Eur. Ceram. Soc*. **20** (2000) 2377
20. A. YASUKAWA, S. OUCHI, K. KANDORI and T. ISHIKAWA, *J. Mater. Chem*. **6** (1996) 1401
21. S. SPRIO, G. PEZZOTTI, G. CELOTTI, E. LANDI and A. TAMPIERI, *J. Mater. Res*. **20** (2005) 1009
22. L. BERTINETTI, A. TAMPIERI, E. LANDI, G. MARTRA and S. COLUCCIA, *J. Eur. Ceram. Soc*. **26** (2006) 987